Supporting Information

Zhang et al. 10.1073/pnas.1018493108

SI Materials and Methods

Cell Culture. Experiments were performed with mouse MC3T3-E1 osteoblasts, mouse ATDC5 chondrocytes, and mouse NIH 3T3 fibroblasts. MC3T3-E1 clone 4 cells (American Type Culture Collection) were maintained and differentiated for 28 d, as described previously (1). Cells were harvested at the indicated times for alkaline phosphatase (ALP) enzyme assays or histochemical detection of ALP (2). ATDC5 cells were grown in DMEM/F-12 (Invitrogen) containing 2% FBS (HyClone). In differentiation conditions, cells were cultured until confluent and then incubated for 2 wk in the same medium supplemented with 10 μg/mL insulin, 10 μg/mL transferrin, 3×10^{-8} M sodium selenite, and 37.5 μg/mL ascorbate 2-phosphate (Fisher). Calvarial osteoblasts were isolated from neonatal mice and maintained as described previously (3).

Reporter Constructs and Antibodies. Mouse Runx2 3′UTR regions were generated by direct PCR amplification from mouse genomic DNA. The gel-purified PCR fragments were cloned into the SpeI/MulI backbone of the pMIR-REPORT microRNA (miRNA) expression reporter (Ambion). The pMIR-REPORT vector contains a CMV promoter that drives expression of the firefly luciferase (LUC) gene and permits insertion of 3′UTRs with miRNA seed sequences through a 3′ polylinker followed by an SV40-derived polyadenylation site. We inserted the ∼4-kbp full-length 3′UTR of Runx2 mRNA (FL-Rx2UTR) as well as two 500-bp regions spanning either a proximal 3′UTR fragment (Prox-Rx2UTR) or a distal 3′ UTR fragment (Dist-Rx2UTR). The latter two each contain clusters of miRNA seed regions (see Figs. 1*A* and 3). The amplification primers used for the generation of the three fragments are shown in Table S1. The constructs were sequenced to ensure accuracy of the cloning procedure (4–6).

Antibodies used in this study include a Runx2 mouse monoclonal antibody (MBLInternational) and β-actin antibody (Santa Cruz Biotechnology).

Transfection Assay. miRNAs, miRNA inhibitors (anti-miRNAs), and miRNA/anti-miRNA negative control no. 1 (obtained from Ambion) were transfected into MC3T3-E1 or mouse primary calvarial osteoblasts at 50% confluence at a concentration of 50 nM with Oligofectamine (Invitrogen). Cells were harvested 72 h after transfection for protein and mRNA analysis. For LUC activity analysis, miRNAs (50 nM) and reporter plasmids (100 ng) were cotransfected into cells with Lipofectamine 2000 (Invitrogen) for 48 h. The Dual-Luciferase Reporter Assay System (Promega) was used to quantify LUC activity. Each value from the *firefly* LUC assay was normalized to the *Renilla* LUC assay value from the cotransfected phRL-null vector (Promega).

mRNA Decay Assays. Stability of mRNAs was examined by treating cells with the general RNA polymerase inhibitor actinomycin D (Sigma) to prevent synthesis of new transcripts. MC3T3-E1 osteoblasts were transfected with nonspecific (NS) miRNAs miR-30c and miR-133a. After 48 h of transfection, actinomycin D (10 μg/mL) was applied in cells, and cells were collected at 0, 1, 2, 4, and 8 h after treatment for mRNA isolation and RT–quantitative PCR (RT-qPCR) analysis (7, 8).

RNA Isolation and Analysis. Total RNA was isolated from cultures of cells by using TRIzol reagent (Invitrogen) according to the manufacturer's protocol. After purification with DNA-free RNA column purification kits (Zymo Research), RNA (1 μg) was then reverse transcribed using the SuperScript First Strand Synthesis Kit (Invitrogen) or the QuantiMir RT Kit (System Biosciences) according to the manufacturer's instructions. The relative expression of a panel of genes was assessed by real-time qPCR. Primer Express software was used to predict optimum RT-PCR primer sets (Table S1), except for GAPDH primers (Applied Biosystems). Specific miRNA forward primers (Table S1) and the 3′ universal primer (provided by the QuantiMir RT Kit) were used for endogenous miRNAs analysis. qPCR was performed with SYBR Green Master Mix (Applied Biosciences) and a two-step cycling protocol (anneal and elongate at 60 °C, then denature at 94 °C). Specificity of primers was verified by dissociation of amplicons using SYBR Green as a detector. All transcript levels were normalized to that of mouse GAPDH or U6 snRNA transcript levels (for miRNA expression).

Statistical Analysis. The data for both the control and experimental groups are presented as means ± SE. Statistical significance was assessed with the Student's t test, and P values <0.05 were considered statistically significant.

1. Zhang Y, et al. (2009) Co-stimulation of the bone-related Runx2 P1 promoter in mesenchymal cells by SP1 and ETS transcription factors at polymorphic purine-rich DNA sequences (Y-repeats). *J Biol Chem* 284:3125–3135.
2. Lengner CJ, et al. (2004) Primary mouse embryonic fibroblasts: A model of mesenchymal cartilage formation. *J Cell Physiol* 200:327–333.
3. Pratap J, et al. (2003) Cell growth regulatory role of Runx2 during proliferative expansion of preosteoblasts. *Cancer Res* 63:5357–5362.
4. O'Donnell KA, Wentzel EA, Zeller KI, Dang CV, Mendell JT (2005) c-Myc-regulated microRNAs modulate E2F1 expression. *Nature* 435:839–843.
5. Behm-Ansmant I, et al. (2006) mRNA degradation by miRNAs and GW182 requires both CCR4:NOT deadenylase and DCP1:DCP2 decapping complexes. *Genes Dev* 20: 1885–1898.
6. Kolachala VL, et al. (2010) Adenosine 2B receptor expression is post-transcriptionally regulated by microRNA. *J Biol Chem* 285:18184–18190.
7. Zhou L, Qi X, Potashkin JA, Abdul-Karim FW, Gorodeski GI (2008) MicroRNAs miR-186 and miR-150 down-regulate expression of the pro-apoptotic purinergic P2X7 receptor by activation of instability sites at the 3′-untranslated region of the gene that decrease steady-state levels of the transcript. *J Biol Chem* 283:28274–28286.
8. Schmittgen TD, et al. (2000) Quantitative reverse transcription-polymerase chain reaction to study mRNA decay: Comparison of endpoint and real-time methods. *Anal Biochem* 285:194–204.

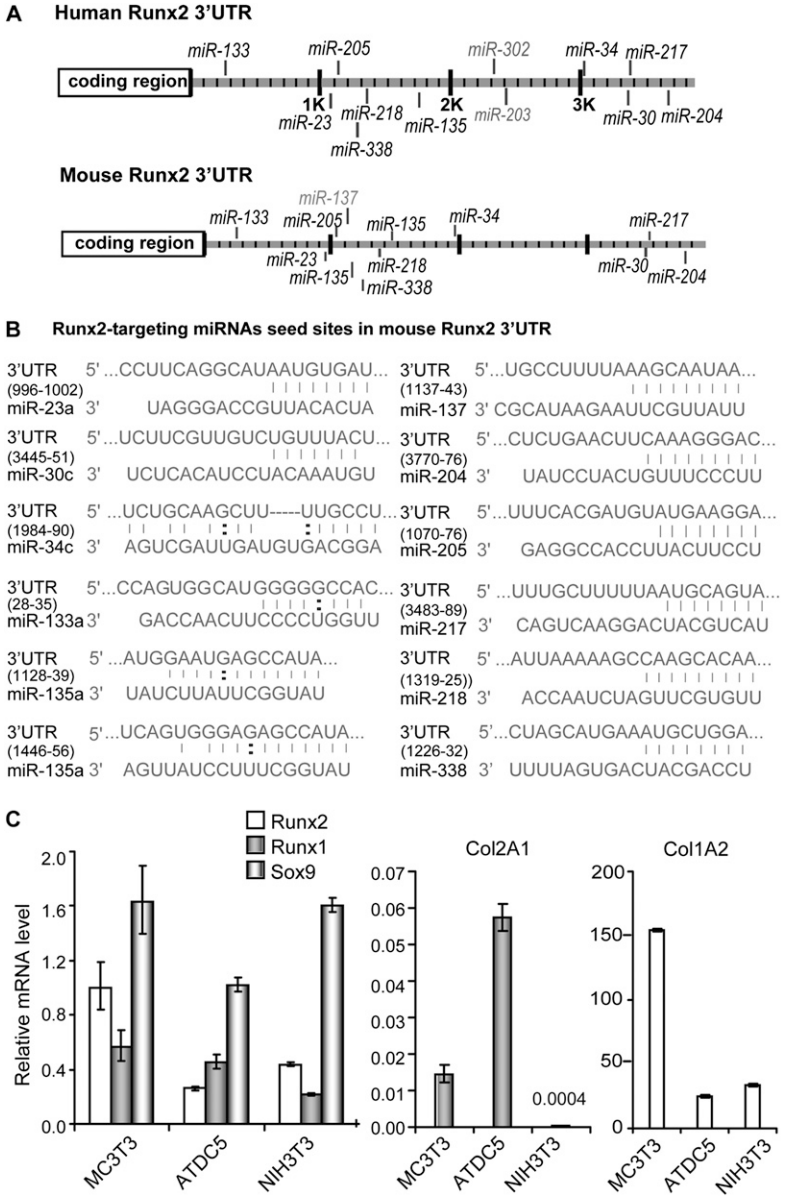

Fig. S1. (*A*) The diagram shows putative miRNA seed sequence locations in the human and mouse Runx2 3′UTRs. Twelve miRNAs were predicted by three programs (TargetScan, PicTar, and RNA22) to target the human Runx2 3′UTR, and 11 miRNAs target the mouse Runx2 3′UTR. Ten of these miRNAs are in common between mouse and human. (*B*) Alignment of our panel of miRNAs predicted to target the mouse Runx2 3′UTR with the mouse Runx2 mRNA shows complementary pairing. (*C*) All three cell lines expressed characteristic cell-type–specific markers. The Runx2 level in MC3T3-E1 was set as 1.

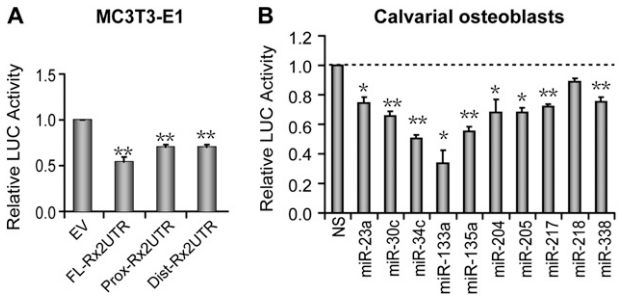

Fig. S2. (*A*) The 3′ UTR of Runx2 mRNA (FL-Rx2UTR, Prox-Rx2UTR, and Dist-Rx2UTR) and the corresponding empty vector (EV) were each transfected into MC3T3 cells. At 48 h after transfection, lysates were harvested for LUC assays. Each of the 3′ UTR segments inhibits reporter activity through miRNAs that are endogenously expressed in MC3T3-E1 cells. (*B*) The effects of Runx2-targeting miRNAs on Runx2 3′ UTR reporter activity in mouse primary calvarial osteoblast. Ten miRNAs were cotransfected with the full-length Runx2 3′ UTR reporter (FL-Rx2UTR) in calvarial osteoblasts. After 48 h, reporter activities were detected by LUC assays. Specific miRNAs repress full-length LUC reporter activity, compared with NS miRNA. Values represent means ± SE ($n = 3$). *$P < 0.05$ and **$P < 0.01$, statistical significance compared with the control group treated with the empty vector or the NS miRNA.

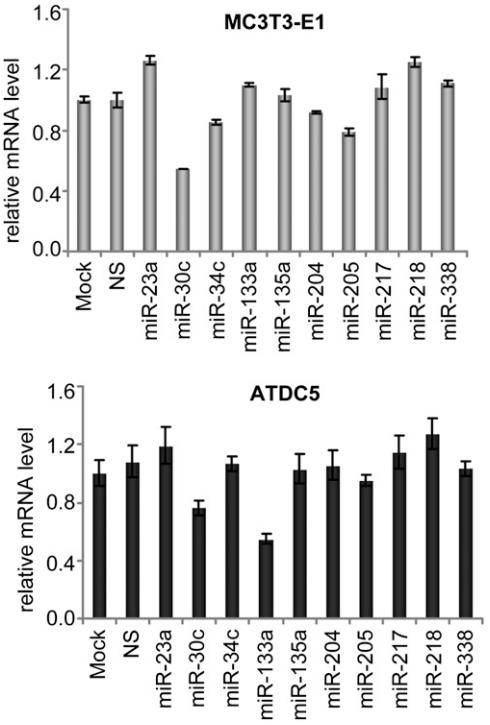

Fig. S3. The majority of Runx2-targeting miRNAs have no or limited effects (less than twofold) on Runx2 mRNA levels upon transfection into MC3T3-E1 or ATDC5 cells. One exception is miR-30c, which suppresses Runx2 mRNA by approximately twofold in MC3T3 cells, and the other exception is miR-133a, which reduces Runx2 mRNA levels by approximately twofold only in ATDC5 cells. RNA samples were collected 72 h after transfection for mRNA analysis with quantitative RT-PCR. The expression levels for Runx2 were normalized to values for GAPDH. The normalized values are presented relative to the Mock group value (set as 1). Values represent means ± SE ($n = 3$).

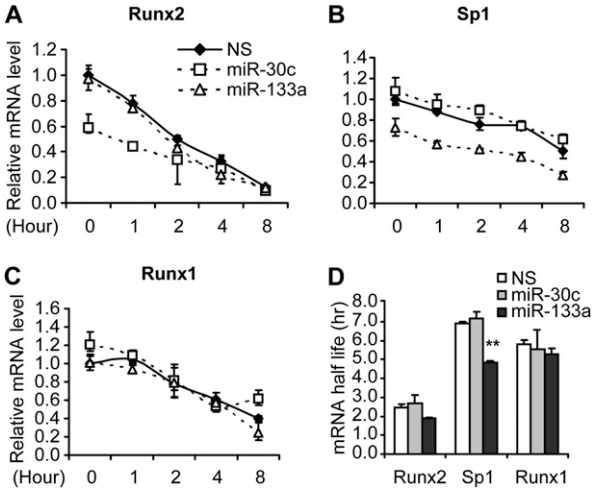

Fig. S4. Effects of miR-30c and miR-133a on mRNA decay in MC3T3 osteoblasts. At 48 h after transfection with miRNAs, cells were treated with actinomycin D (10 μg/mL) for 1, 2, 4, and 8 h. The levels of several mRNAs, including Runx2 (*A*), Sp1 (*B*), and Runx1 (*C*), were monitored by RT-qPCR. miR-133a did not change the Runx2 mRNA level. Although miR-30c showed 50% repression of Runx2 mRNA level, it did not affect mRNA half life (*D*). Sp1 is predicted to be the target of miR-133a but not of miR-30c. Thus, miR-30c had no effect on Sp1 gene expression. miR-133a inhibited Sp1 gene expression and also reduced Sp1 mRNA half life. Both miR-30c and miR-133a did not change Runx1 mRNA level or half life. The gene expression levels were normalized to values for GAPDH and are presented relative to the NS miRNA group value at 0 h (set as 1). Values represent means ± SE ($n = 3$). $^{**}P < 0.01$, statistical significance compared with the control group treated with the NS miRNA.

Table S1. Nucleotide sequences of primers for cloning and qRT-PCR

Name	Type of primer	Primers (5′ to 3′)
Reporter constructs		
FL-Rx2UTR	Cloning	Forward: GAG ACT AGT AAA TTC GTC AAC CAT GGC
	Cloning	Reverse: CAA ACG CGT GAA AAA AAA AGC CTT TTT A
Prox-Rx2UTR	Cloning	Forward: GAG ACT AGT TTG ACT TCG GTC TCT AAA AGT GTG
	Cloning	Reverse: CAC ACG CGT TGC AAT TTA GAG TTT TGC TCA ACT
Dist-Rx2UTR	Cloning	Forward: GAG ACT AGT ACC TAG TTA GAG TGG TAG CAG AAG
	Cloning	Reverse: CAC ACG CGT ATC ATG AGA GGG GGA AAT GCC A
Bone marker genes		
Runx2	qRT-PCR	Forward: CGG CCC TCC CTG AAC TCT
	qRT-PCR	Reverse: TGC CTG CCT GGG ATC TGT A
ALP	qRT-PCR	Forward: CCA ACT CTT TTG TGC CAG AGA
	qRT-PCR	Reverse: GGC TAC ATT GGT GTT GAG CTT TT
Osteocalcin	qRT-PCR	Forward: CTG ACA AAG CCT TCA TGT CCA A
	qRT-PCR	Reverse: GCG CCG GAG TCT GTT CAC TA
Osteopontin	qRT-PCR	Forward: ACT CCA ATC GTC CCT ACA GTC G
	qRT-PCR	Reverse: TGA GGT CCT CAT CTG TGG CAT
Sox9	qRT-PCR	Forward: GAGGCCACGGAACAGACTCA
	qRT-PCR	Reverse: CAGCGCCTTGAAGATACGATT
Col1A1	qRT-PCR	Forward: GCT CCT CTT AGG GGC CAC T
	qRT-PCR	Reverse: CCT TTGTCA GAA TAC TGA GCA GC
Col2A1	qRT-PCR	Forward: CTGGAATGTCCTCTGCGA
	qRT-PCR	Reverse: TGAGGCAGTCTGGGTCTTCAC
Runx1	qRT-PCR	Forward: CCAGCAAGCTGAGGAGCGGCG
	qRT-PCR	Reverse: TGACGGTGACCAGAGTG
Sp1	qRT-PCR	Forward: ATCTGGTGGTGTGGGATACA
	qRT-PCR	Reverse: GAGGCTCTTCCCTCACTGTCT
Mature miRNA		
miR-23a	qRT-PCR	ATC ACA TTG CCA GGG ATT TCC
miR-30c	qRT-PCR	TGT AAA CAT CCT ACA CTC TCA GC
miR-34c	qRT-PCR	AGG CAG TGT AGT TAG CTG ATT GC
miR-133a	qRT-PCR	TTG GTC CCC TTC AAC CAG CTG T
miR-135a	qRT-PCR	TAT GGC TTT TTA TTC CTA TGT GA
miR-137	qRT-PCR	TAT TGC TTA AGA ATA CGC GTA G
miR-204	qRT-PCR	TTC CCT TTG TCA TCC TAT GCC TG
miR-205	qRT-PCR	TCC TTC ATT CCA CCG GAG TCT G
miR-217	qRT-PCR	TAC TGC ATC AGG AAC TGA CTG GAT
miR-218	qRT-PCR	TTGTGCT TGA TCT AAC CAT GT
miR-338	qRT-PCR	TCC AGC ATC AGTGAT TTT GTT GA
Control		
GAPDH	Control	Forward: AGG TCG GTG TGA ACG GAT TTG
	Control	Reverse: TGT AGA CCA TGT AGT TGA GGT CA
U6	Control	Forward: CGC TTC GGC AGC ACA TAT AC
	Control	Reverse: AAA ATA TGG AAC GCT TCA CGA